Improving Separation Performance of PVDF Ultrafiltration Membranes by Blending with Cellulose Acetate

Reza, Muhammad*[+]
Department of Chemistry Education, Universitas Islam Negeri Ar-Raniry Banda Aceh, 23111, INDONESIA

Pramono, Edi
Department of Chemistry, Universitas Negeri Sebelas Maret, Surakarta, 57126, INDONESIA

Radiman, Cynthia L.
Inorganic and Physical Chemistry Division, Institut Teknologi Bandung, Bandung, 40132, INDONESIA

ABSTRACT: *Membrane technology is a clean technology for various separation processes, in which additional waste products are not produced. Poly(vinylidene fluoride) (PVDF) is one of the synthetic polymers widely used as commercial ultrafiltration membranes. Unfortunately, this polymer is hydrophobic and consequently, it has low flux in the aqueous system and creates fouling phenomena on the surface of the membrane. Therefore, the objective of this work is to improve the hydrophilicity of PVDF membranes by preparing blend membranes using cellulose acetate. Cellulose Acetate (CA) with varied concentrations ranging between 1 and 10 wt.% were added to poly(vinylidene fluoride) and those blend membranes were prepared via the phase inversion method. The effects of CA on various membrane characteristics such as hydrophilicity, membrane porosity, antifouling properties, and separation performances were investigated using Methylene Blue (MB) as a dye. It was found that the PVDF-CA membranes were more hydrophilic compared to the pristine PVDF membrane, revealed by the decrease of water contact angle from 72.93˚ to 56.43˚ along with CA addition. The water flux increased with CA concentration; its value reached 132.95 L/m^2 h for blend membranes with 5% CA. Moreover, this composition also exhibited the optimum MB rejection of 90.24%. Furthermore, the improvement of hydrophilicity increased the antifouling properties, indicated by the increase of Flux Recovery Ratio (FRR) from 45-96%, the decrease of irreversible fouling from 60-3%, and the improvement of reversible fouling from 10-55%.*

KEYWORDS: *Poly(vinylidene fluoride); Cellulose acetate; Phase inversion; Ultrafiltration membrane; Fouling properties.*

INTRODUCTION

The membrane has an important role in chemical technology. It has been widely used for several applications, such as the production of clean water, reduction of pollutants, and removal of toxic or worth compounds

***** *To whom correspondence should be addressed.*
+ E-mail: muhammad.reza@ar-raniry.ac.id
1021-9986/2023/3/1006-1018 13/$/6.03

from industrial liquid waste [1]. The factors that affect the improvement of membrane technology utilization is high efficiency of separation, low energy consumption, simplicity, and soft operation system [2, 3].

In recent years, poly (vinylidene fluoride) (PVDF) has become popular to be used for membrane material. It finds application for water treatment and separation processes due to beneficial properties such as high mechanical and thermal stability, and resistance to chemical degradation [4]. PVDF, a semi-crystalline polymer, has been applied to synthesize membranes using Loeb-Sourirajan inversion phase method [5]. However, the hydrophobicity of PVDF renders low properties for both permeability and antifouling to microporous PVDF membrane [6].

Since the PVDF is hydrophobic, thus the membranes have low permeability. There are many ways conducted to increase membrane performance either permeability or selectivity, which are physical blending and surface modification [7]. Blending is the most practical method to modify polymeric membranes and can be used on an industrial scale [4]. Various techniques for blending are the addition of hydrophilic polymers, surface modification, and composite production with hydrophilic inorganic materials [8]. The addition of hydrophilic polymers is very easy and has successfully enhanced the performance of PVDF ultrafiltration membranes [9–13]. Some blended membranes have higher permeability, and selectivity, and are more hydrophilic, and they have been used for membrane separation applications like UltraFiltration (UF) and MicroFiltration (MF) [14]. In addition, Blended membranes have permeability which is 5-10 times greater than pristine PVDF membranes [15]. Another research revealed that the permeability of blended PVDF membranes was enhanced extremely, showed by the permeate flux of 1266.5 L m^{-2} h [16].

The blending method is not only used to increase the permeability, but also to reduce the fouling that occurred during practical filtration, and it decreased the water flux, permeate flux, and separation efficiency. The addition of functional additives results in higher hydrophilicity and antifouling properties. Blended PVDF membranes have a Flux Recovery Ratio (FRR) of 88.5%, indicating excellent antifouling properties [17]. The introduction of hydrophilic membranes to PVDF surface improved antifouling properties and Flux Recovery Ratio (FRR) by about 19 and 10%, respectively [18]. Another study reported that 89% of fouling on PVDF membrane surface was easily removed by the blending method [19], and overall this method produced blended PVDF membranes with antifouling properties at the optimum blending ratio [15].

Cellulose acetate (CA) is used as a blending agent in this study because it is easily produced by acetylation of cellulose which is the most abundant natural polymer on earth. There are many excellent properties of CA such as low price, good biocompatibility, high hydrophilicity, and environmental friendly product form sustainable resources [20]. The hydrophilicity of cellulose is potentially to be used for application in PVDF membrane. In the previous study, PVDF modification by the addition of nanocrystal cellulose produced a membrane with good antifouling properties in Bovine Serum Albumin (BSA) separation [21]. Other research also found that the CA-polysulfone blend ultrafiltration membrane has higher permeability and hydrophilicity. The presence of polymer produced from cellulose acetylation, cellulose acetate (CA) as an additive, yielded a membrane with strongly higher permeability compared to pristine PVDF membrane [22]. Besides that, it has a high rejection with a percentage which is greater than 90% for the removal of BSA [6, 23]. However, the use of CA composition above 20% increased the total fouling, indicated by the increase of irreversible fouling and the decrease of reversible fouling [23]. A further study reported that to overcome the lack of fouling properties at 20% composition, it used other additives inside a coagulant bath [24]. At a higher composition of CA which is above 10%, the rejection of PVDF/CA membranes was below 90% [25]. Therefore, in this study, the average CA composition below 10% is used to find out the separation performance and antifouling properties. Besides that, the excellent properties of the blended polymeric membrane of PVDF-CA have never been used for dye ultrafiltration applications.

In addition, in this present study, CA was used as an additive in PVDF membranes. The effect of blending CA with PVDF on permeability, hydrophilicity, porosity, morphology and antifouling was evaluated. The main objective of our study was to investigate the separation performance of PVDF-CA membrane to form membrane with high permeability and selectivity. To investigate the separation performance, Methylene Blue (MB) is used for filtration experiments.

EXPERIMENTAL SECTION

Reagents

Poly (vinylidene fluoride) (PVDF) powder (Solef® 1015) was supplied by Solvay. Cellulose Acetate (CA) (MW=30,000 Da) was purchased from Sigma Aldrich. N,N-dimethylacetamide (DMAc) (99%, Merck) from Singapore was used as solvent. Dextran T-500 (MW=500 kDa) from Pharmacosmos was used for pre-treatment analysis. Distilled water was used as non-solvent in coagulant bath. Sulfuric acid (H_2SO_4) (95-97%, Merck) was obtained from Singapore. Methylene blue ($C_{16}H_{18}ClN_3S$. xH_2O, 319.85 g/mol, Merck) was used for dye ultrafiltration.

Membrane fabrication

The PVDF/CA blend membranes were fabricated *via* phase inversion method. PVDF and CA (with various concentration ratios) were dissolved in DMAc at 60 °C. The mixture was continuously stirred for 24 h to ensure the polymers were completely dissolved. The casting solution was then degassed for 4 h without stirring to allow complete release of bubbles. Afterward, the solutions were cast on glass plate and immediately immersed into coagulant bath containing distilled water at room temperature. The fabricated membranes were washed thoroughly with deionized water to remove residual solvent, and then kept in water before testing. The composition of casting solution was given in Table 1. This polymer composition is properly to be used based on previous study that results the stronger mechanical properties between 17-19% [26]. The lifetime of membranes is supported by the mechanical strength to avoid

\the fracture during filtration.

Permeability and selectivity

The permeability was evaluated using the filtration method. The filtration of membranes was examined using a dead-end ultrafiltration cell. Initially, membranes with diameter of 5 cm were washed with distilled water to remove residual glycerin. Each membrane was compacted at 2 bars by passing distilled water for 30 min. The water flux (J_w) was calculated using the equation below [27].

$$\mathrm{J_w} = \frac{\mathrm{V}}{\mathrm{A\,x\,t}} \quad (1)$$

where V is the volume of collected permeate, A is the membrane area, and t is the permeation time.

Table 1: Dope composition of PVDF/CA membranes.

Polymers (18 wt%)		Solvent, DMAc (wt%)
PVDF	CA	
100	0	82
99	1	82
97	3	82
95	5	82
90	10	82

Dye filtrations were provided to analyze the antifouling properties of membranes. The 1000 ppm of methylene blue solution was passed under 2 bars for 30 min, and the flux of dye solutions were recorded as J_p. Afterwards, the membranes were washed with deionized water for 5 min for further experiment called back-washed treatment and the flux was again calculated. This step was popularly known as flux recovery ratio (FRR) and the FRR of membranes was determined using the equation [28].

$$\mathrm{FRR} = \frac{\mathrm{J_R}}{\mathrm{J_w}}\ \mathrm{x}\ 100\% \quad (2)$$

Where J_R is recovery flux of membranes after filtration with dye solution and J_w is water flux during compaction period.

During filtration experiments, the permeate and concentrate (feed) of methylene blue were collected and measured. The selectivity of the membrane was represented by percent rejection. The concentration of dye solutions in concentrate and permeate solutions was determined by spectrophotometry method using a UV-Visible spectrophotometer (EVOLUTION 220). For Methylene Blue (MB) solutions, the analysis was conducted at 665 nm [29]. The rejection (R), total fouling rratio (R_t), reversible fouling ratio (R_r), and irreversible fouling ratio (R_{ir}) were calculated as follows [30].

$$\mathrm{R} = \frac{\mathrm{C_0 - C_1}}{\mathrm{C_0}}\ \mathrm{x}\ 100\% \quad (3)$$

$$\mathrm{R_t} = \frac{\mathrm{J_w - J_P}}{\mathrm{J_w}}\ \mathrm{x}\ 100\% \quad (4)$$

$$\mathrm{R_r} = \frac{\mathrm{J_R - J_P}}{\mathrm{J_w}}\ \mathrm{x}\ 100\% \quad (5)$$

$$\mathrm{R_{ir}} = \frac{\mathrm{J_w - J_R}}{\mathrm{J_w}}\ \mathrm{x}\ 100 \quad (6)$$

Porosity and Pore size measurement

The membrane porosity was measured by gravimetric method. Initially, membranes were immersed into distilled water for 4 h at room temperature. Afterward, wet membranes were weighed using analytical balance after carefully wiped the surface with tissue. These wet membranes were dried at 60 ℃ for 24 h. Then, the dry membranes were weighed again. The membrane porosity was calculated using the equation below [31].

$$\varepsilon = \frac{W_w - W_d}{\rho_w A l} \quad (7)$$

where W_w is weight of wet membrane, g; W_d is weight of dry membrane, g; ρ_w is water density at room temperature, g cm^{-3}; A is membrane area, cm^2; and l is wet membrane thickness, cm.

To identify the membrane pore size, the experiment used bubble-point method. By using this method, the biggest pore diameter can be observed according to pressure that used to produce air bubble on the membrane surface moistened by water. The radius of pore (r_p) was determined using the following equation [3].

$$r_p = 2\frac{\gamma}{\Delta P}\cos\theta \quad (8)$$

Where γ is water surface tension (72.8 mJ/m^2 at room temperature); ΔP is pressure deviation from starting point; and θ is the contact angle which is 0 represented between membrane surface and water.

Water contact angle

The surface hydrophilicity of membranes were analyzed by measuring the angle between meniscus resulted by water and membrane surface using water contact angle-meter (θ). The flat membranes were put on sample holder and then were dropped by deionized water on the membrane surface using Mitutoyo sessile drop. After the images were recorded, the contact angle was calculated using ImageJ (https://imagej.nih.gov/ij/) software with contact angle plugin. The average of at least 3 measurements was reported. The solid-liquid interfacial free energy of hydration of membranes was determined using Young-Dupré equation as follows [32].

$$-\Delta G_{SW} = (1 + \cos\theta)\gamma_w \quad (9)$$

where θ is the average contact angle and γ_w is water surface tension (72.8 mJ m^{-2} for deionized water at room temperature). The hydrophilicity of membranes can be quantified by calculating the free energy of hydration (ΔG_{SW}) [33].

Crystalline phase

The crystalline phase of membranes was study using ATR-FT-IR (Fourier Transform Infrared) (Alpha Bruker). The measurement was conducted at range of 500 to 1000 cm^{-1}. The crystalline phase was represented by β-phase and it was calculated using the following equation.

$$F(\beta) = \frac{P_\beta}{1.26P_\alpha + P_\beta} \quad (10)$$

where $F(\beta)$ is the mass fraction of β-phase in PVDF polymer, P_α and P_β are the absorption peaks of α and β phases regarding to wave numbers of 763 and 840 cm^{-1} respectively [34].

Mechanical strength and morphology

Before tested, the wet membranes were patterned to be 50 mm x 2.5 mm and the thickness was measured using Mitutoyo thickness gages. The mechanical strength tests conducted using Textechno Favigraph with a 5 kN load cell and constant speed of 10 cm/min at room temperature. For supplementary analysis, the shrinkage test was conducted by measuring the wet membrane area (A_w) and after drying (A_d) at room temperature. The reduction of membrane thickness can be ignored compared to contraction in membrane area. Afterwards, the shrinkage (S) was represented by percentage reduction in membrane area after drying and it was calculated as follows [34].

$$S = \frac{A_w - A_d}{A_w} \text{ x } 100 \quad (11)$$

The morphology analysis involved surface and cross section of membrane structures was observed using Scanning Electron Microscope (SEM) (HITACHI SU3500).

RESULTS AND DISCUSSION

Water contact angle

Water contact angle measurements are usually conducted to indicate the hydrophilicity of membranes. The water contact angle observed at zero of operational time is called as static contact angle. Fig. 1 showed the static water contact angle of membranes surface

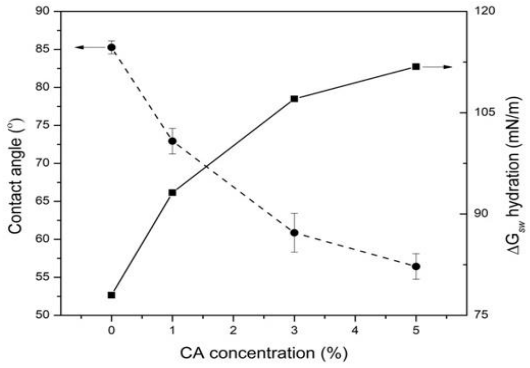

Fig. 1: The influence of CA addition to water contact angle and dynamic free energy of various membranes.

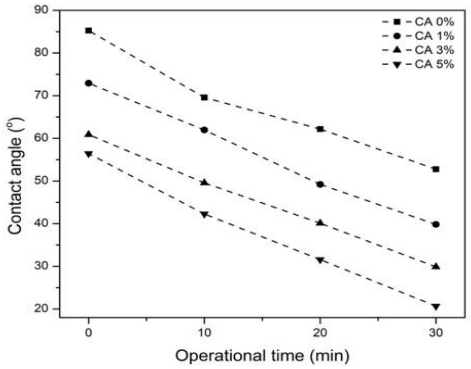

Fig. 2: The summary of dynamic contact angles of various membranes for 30 minutes.

with the different of CA addition. The pristine PVDF membrane has the biggest water contact angle of 85.27˚, indicating the highest hydrophobicity among the blend membranes. The water contact angle decreased from 72.93˚ to 56.43˚ along with CA addition. However, the measurement of static contact angle is not proper for microporous membranes. Due to the immiscibility of PVDF and CA, the microporosity is created during phase inversion. Thus, the PVDF/CA membranes will have various condition of smooth and rough surface area. The more CA composition, the membranes surface will be rougher. So, the water drop will be penetrated continuously into micropores due to capillary force [35]. The measurement of dynamic contact angle is more accurate to determine the decrease of water contact angle with the operational time as shown in Fig. 2.

The initial contact angles of blend membranes were gradually decreased with addition of CA in membranes, and the initial contact angle of composite membranes are smaller than pristine PVDF membrane. The dynamic contact angles were slowly decreased for 30 minutes. Since the pristine PVDF membrane is very hydrophobic according to static contact angle, but the dynamic contact angle is still decreased about 32 ˚ during operational time. The reduction is occurred because of the formation of microporosity on the membrane surface. Besides that, the highest reduction is showed by membranes with 5% of CA. However, the decrease of dynamic contact angle for membranes with 1 and 3% CA addition is similar with pristine PVDF membranes. This finding proved that the main factor affecting water contact angle is microporosity of membranes [36].

The microporosity of membranes is not only influence the water contact angle, but also the interaction between membranes surface and water. Thermodynamically, the interaction can be calculated mathematically using Gibbs free energy of hydration ($-\Delta G_{sw}$). The higher Gibbs energy of hydration, the interaction between membranes surface and water will be stronger. As shown in Fig. 1, the blend membranes had higher value of $-\Delta G_{sw}$ than pristine PVDF membrane. The Gibbs free energy of hydration is improved from 78 to 113 mN/m along with CA addition. This is revealed that the interaction is occurred spontaneously. In addition, the results exhibited that the addition of CA in membranes increased the membrane hydrophilicity.

Crystalline phase

Surface hydrophilicity was also supported by the crystalline phase of membrane structure. The crystalline phase was computationally determined according to ATR-FT-IR analysis and the data is shown in Fig. 3. The β-phase of various membranes was affected by the CA content in the blend membranes. The value of β fraction explained the crystalline mass of PVDF in membranes. Pristine PVDF membrane has the lowest F(β) 0% and the composition 5% CA has the highest F(β) which is 94%. The crystalline phase of membranes was represented by polymorphism and is well known to crystalline in different forms of α and β. The β is readily formed when the casting solution was cooled to produce crystal structure form the melt [37]. The improvement of CA content in blend membranes exhibited the faster formation to reach crystal structure. Via cooling section, the presence of CA helped

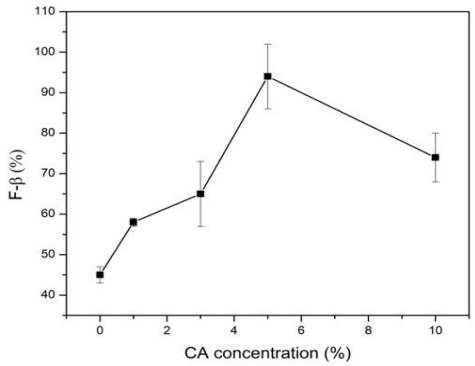

Fig. 3: Membrane β-phase mass fraction, F(β).

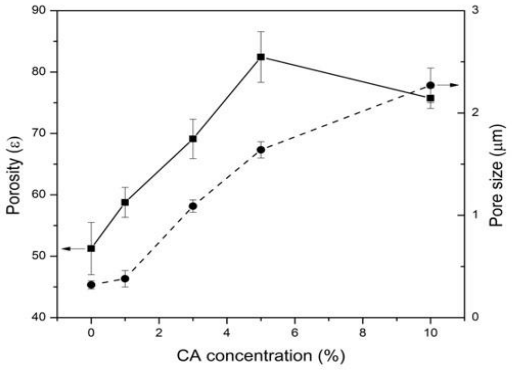

Fig. 4: The effect of CA addition on the porosity and pore size of membranes.

the formation of the crystalline phase of polymeric membranes. CA polymer has a polar functional group which renders the structure more rigid than PVDF in general. It is very relevant to data in this study, the more CA content introduced to the membrane, the higher F(β) obtained. In addition, the formation of the crystalline phase influenced the mechanical strength of the polymer [38].

Porosity and pore size

Bulk porosity of membranes was determined using the gravimetric method and the data is shown in Fig. 4. The value of bulk porosity was obtained in the range of 50 to 80%. The bulk porosity increased along with CA addition in blend membranes. However, the value decreased when 10% CA to blend membrane because of its dense morphology. As explained before in Fig. 1, the membrane permeability increased till the membrane with the composition of 5% CA, but decreased after adding 10% CA. Generally, it indicates that membranes with higher porosity generate higher flux. The CA content in membranes decreased from top to bottom surface [39]. There are several parts of CA dissolved into non-solvent during the phase inversion process, resulting in larger and more pores on the top surface.

The result of the pores size measurement is also presented in Fig. 4. The biggest pore size increased along with CA addition. Briefly, the addition of composite affected the distribution of membrane pore size [40]. Compared to the data on membrane pore size, the porosity has a different trend with membrane pore size. But, this phenomenon explains that the increase of porosity will not surely followed by the increasing of pore size. Because this method was only used to measure the biggest pore size, thus it will not confirm the pore distribution on membrane surface. On other hand, this condition supported the permeability and selectivity data represented in Fig. 5. The decline of water flux and rejection to dextran T-500 were attributed by membrane pore size. According to the results, the water permeability was primary affected by membrane porosity rather than surface hydrophilicity.

Filtration and antifouling properties

The water permeability of the blend membranes was calculated as water flux, and it was represented by J_w. For pre-treatment test, it used to evaluate the influence of blending composition on membrane performance and selectivity to neutral compound (dextran T-500), and data are presented in Fig. 5. The water flux of the membranes increased along with CA concentration in the membranes. Its value achieved 137.61 L/m^2.h and decreased when added 10% of CA. The presence of CA could improve the hydrophilicity and porosity of membranes. Hence, the membrane had the highest water flux for blend membrane with 5% of CA. However, as the CA increased in the membrane, the water flux slightly decreased. This condition probably affected by the formation of dense structure of membrane with 10% CA (as shown in Fig. 10). Clearly, the composite membranes exhibit the greater water flux, which is affected by increase of surface hydrophilicity, or the increase of pore size [41].

As shown in Fig. 1, the rejection for dextran T-500 tends to decrease when the CA composition increased.

The good separation process will be obtained when the percentage of rejection was higher than 90%. The pristine PVDF membrane had the highest rejection of 96.45% and slightly decreased to 92.11, 91.37, and 90.01% respectively. The highest decrease showed by the addition of 10% CA which is 38.07%. The decline of rejection for composition between 1 and 5% CA is still acceptable and considered standardization. The lowest rejection of the membrane might be related to the morphology of the membrane which will be explained in the next section (as shown in Fig. 10). Besides that, the pore size and dimension of the feed solution also affected the rejection of membranes [42], [43].

The permeability of (J_w,J_P, and J_R) of blend membranes to MB was also monitored to analyze the effect of CA composition on the permeation behavior, and the data are shown in Fig. 6. As predicted, the J_P value is lower than J_w and J_R, and the J_P and J_R have the same trend as J_w. The highest J_P reached 83.17 L/m^2 h for MB filtration respectively. These phenomena were caused by the membrane fouling. The separation process and lifetime of the membranes depend on the dynamic properties of fouling. Total fouling ratio, rejection and flux recovery ratio were measured to evaluate the antifouling properties of blend membranes. The total fouling ratio after dye filtration was given in Fig. 7. MB filtration has total fouling which is decreased from 62.25 to 59.57%, the irreversible fouling ratio (R_{ir}) decreased from 61.02 to 4.23%, and reversible fouling ratio (R_r) increased from 11.70 to 55.34%.

Reversible fouling determined the lifetime of membranes for filtration. High reversible fouling ratio can be profitable membranes. Irreversible fouling is impossible to remove by physical cleaning, and by physical treatment only the reversible fouling can be removed. The enhancement of reversible membra ne fouling ratio reached 94% from pristine PVDF membrane to blending membrane with 5% CA during MB filtration. It confirmed that the blend membrane has excellent antifouling properties for dye filtration.

Fig. 6 also illustrates the effect of CA addition to rejection and FRR value of blend membranes can be seen in Fig. 7. The membrane rejection towards MB solutions slightly decreased from 97.80 to 90.24%. It showed the rejection of MB as cationic dye solution is greater than 90%. Previous research reported that PVDF is a membrane

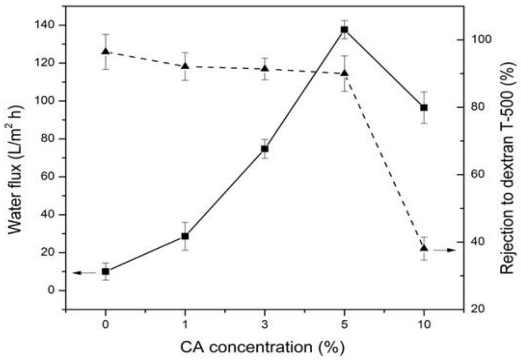

Fig. 5: The influence of CA addition to permeability of various membrane and their rejection to Dextran T-500.

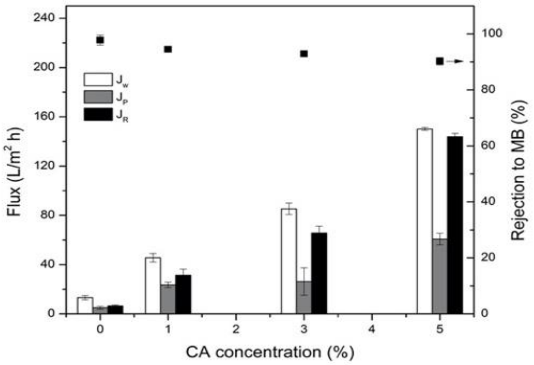

Fig. 6: The permeability (J_w,J_P, and J_R) of pure water and MB solution and MB rejection for various membranes.

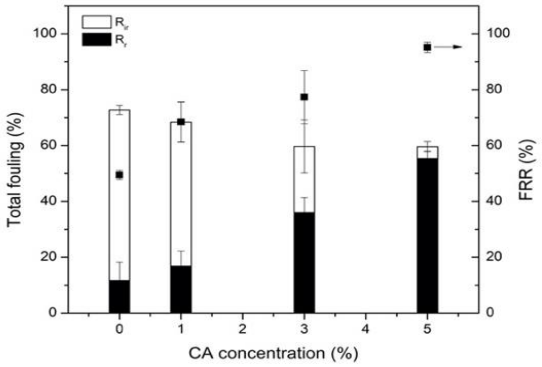

Fig. 7: The summary of R_r and R_{ir} and FRR of the various membranes with MB as the foulant.

Table 2: The comparative studies of PVDF/CA membranes.

Membranes composite	Water fluxes ($L/m^2.h$)	Rejection (%R)	Reversible fouling (%)	Irreversible fouling (%)	References
PVDF/CA 5%	137	97	38	22	This research
PVDF/CA 20%	522	91	20	25	Razzaghi et al., 2014
PVDF/CA/PEG 3%	563	-	-	-	Fitri & Widiastuti, 2017
PVDF/CA 10%	26253	85	-	-	Alias et al., 2020
PVDF/CA/PA 12%	1.1	91.3	-	-	Doung et al., 2016
PVDF/CA 20% + NaCl 584.4 g	248	-	10	12	Razzaghi et al., 2018
PVDF/CA 10%	420	-	-	-	Mu et al., 2010
PVDF/CA 8%	1860	-	-	-	Li et al., 2015

with negatively charged surface according to zeta potential data [42], and so does cellulose acetate [44, 45]. Consequently, the negative charge will automatically supported the interaction between membrane surface and cationic dye solutions to produce high rejection. The highest FRR values for MB solutions obtained 95.77%. On other hand, it can be concluded that the addition of CA as hydrophilic polymer improved the hydrophilicity of blend membranes. Besides that, it also enhanced the antifouling properties of blend membranes. The following (Table 2) is several comparative studies related to the performance of PVDF membranes

Mechanical strength

The mechanical strength is closely related to the membrane structure (*Pang et al*. 2015). The mechanical reduction of blend membranes compared to pristine PVDF is supported by porosity and pore size producing from CA addition in the polymer matrix. As shown in Fig. 8, the tensile strength decreased sharply from pristine PVDF to M3, which is about 40% from 5.59 to 3.01 MPa. Besides that, the elongation at break also decreased about 55% from 158.75 to 72.45%. Due to the good properties of elongation at break of blend membranes, its excellent mechanical strength is promising for blend membranes to be used for dye ultrafiltration process.

The previous study reported that the concentration of PVDF affected the mechanical strength. The highest strain is presented by membrane contained 195 PVDF, which is 148.8%. While the higher concentration of 21% PVDF resulted 91.1% of strain, which is less elastic than 19% PVDF [26]. According to this result, it can be concluded that the elasticity of membrane is mostly affected by PVDF, rather than CA as additive. Therefore, the addition of CA decreased the mechanical strength.

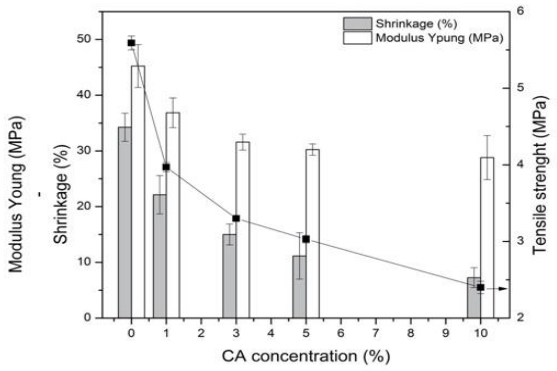

Fig. 8: The effect of CA addition to the mechanical strength of membranes.

The membrane shrinkage affected the performance of membrane mechanical strength [34]. The high tensile strength of pristine PVDF membrane is influenced by the highest membrane shrinkage of about 35%. The shrinkage of membranes was also given in Fig. 8. The presence of hydrophilic polymer in membranes increased the rigidity of membrane structure. Compared to data of elongation at break, the elastic properties of blend membranes were less than pristine PVDF membrane. Therefore, the shrinkage of membranes decreased along with CA addition.

Morphology

Fig. 9 shows the morphology of membranes surface. The pristine PVDF membranes has the smooth surface, whereas the surface become rougher along with CA addition. Composite membrane with 5% of CA has more microporous among other membranes. This surface condition supported the dynamic contact angle (as shown in Fig 5), where the decrease of dynamic contact angle of pristine PVDF membrane is similar with addition of

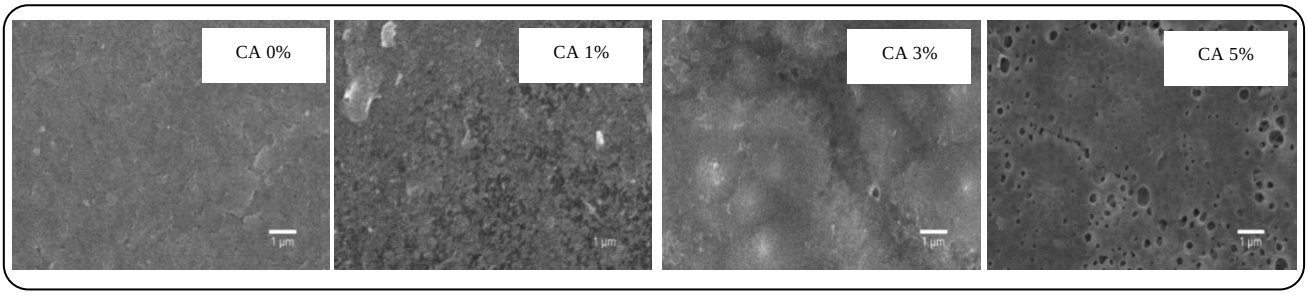

Fig. 9: The effect of CA addition to the membrane roughness.

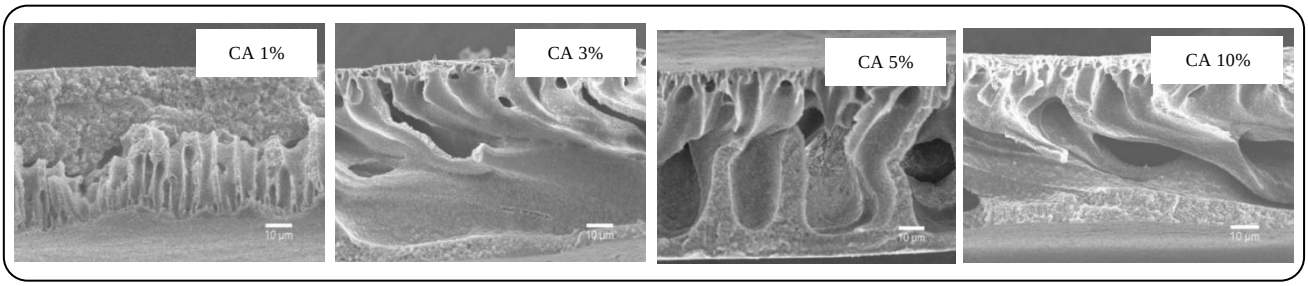

Fig. 10: The cross-sectional morphology of PVDF/CA membranes.

1 and 3% of CA. The result is obtained because the surface roughness of pristine PVDF membrane is similar with composite membranes of 1 and 3% CA addition.

According to Fig. 10, the membranes have the smaller pore on the surface, but the pores become bigger inside the structure. The smaller pores are called as microvoid of sponge-like structures, while the bigger or finger-like structures are called as macrovoid. The sponge-like structures are mostly formed on the top layer, and it affected the hydrophilicity of membranes surface. Then, the hydrophilicity influenced the permeability of membranes. Since the addition of 10% CA decreased the water flux (as shown in Fig. 1), it proved that the permeability of membranes is not only affected by surface hydrophilicity, but also the formation of finger-like structures inside the membranes. The highest water flux is obtained by membrane with 5% CA, because it has the larger macrovoids, while the addition of 10% CA produced smaller macrovoids that results the lower water flux compared to membranes with addition of 5% CA.

The cross-sectional SEM image is also related with membrane porosity (as shown in Fig. 6). Generally, the composite membranes exhibit greater porosity than pure PVDF membrane [46]. The highest porosity is showed by membrane with addition of 5% CA, while the number is reduced when 10% of CA are added into the polymer solution. The phenomena are influenced by the miscibility between polymer and nonsolvent. Since the polymer has high miscibility with nonsolvent, the polymer will lose the larger number of solvents and created high porosity during phase inversion. However, the high concentration of CA in polymer solution made stronger interaction with solvent, so the less of solvent that will be released during phase inversion. This result supported the smaller macrovoids and dense structure formed presented by membranes with addition of 10% CA.

CONCLUSIONS

Blend membranes were prepared with different CA concentrations via phase inversion and characterized by various techniques. The membranes with 5% CA showed the highest porosity and crystalline phase. Then, the water contact angle is decreased along with CA addition, thus the most hydrophilic is showed by surface of PVDF/CA 10% membranes. Nevertheless, the composition of 10% CA reached the greatest surface hydrophilicity, the filtration performance is also supported by membrane porosity, indicated by porosity measurement and SEM image. The composition of 5% CA showed the larger macrovoids than 10% CA. This structure resulted the highest water flux of 132.95 $L/m^2.h$ by membrane with 5% CA.

The composite membrane with the highest water flux also obtained the highest rejection up to 90.24% during MB filtration. In addition, the fouling resistance

of membrane is increased along with CA addition, indicated by the decrease of total fouling from 70-60% and the increase of reversible fouling from 12-58%. The greater improvement of reversible fouling indicated that the addition of CA supported the increase of membrane antifouling properties.

Received : Mar. 10, 2022 ; Accepted : May 30, 2022

REFERENCES

[1] Saljoughi E., Amirilargani M., Mohammadi T., Effect of PEG Additive and Coagulation Bath Temperature on the Morphology, Permeability and Thermal/Chemical Stability of Asymmetric CA Membranes, *Desalination*, **262(1–3)**: 72–78 (2010). doi: 10.1016/j.desal.2010.05.046.

[2] Baker R.W., "Membrane Technology and Application", Second Edition. California: John Wiley & Sons, Ltd, (2004).

[3] Mulder M., "Basic Principles of Membrane Technology". Netherland: Kluwer Academic Publishers, (1996).

[4] Liu F., Hashim N.A., Liu Y., Abed M.R.M., Li K., Progress in the Production and Modification of PVDF Membranes, *Journal of Membrane Science*, **375(1–2)**: 1–27 (2011). doi: 10.1016/j.memsci.2011.03.014.

[5] Tang C.Y., *et al.*, Effect of Solution Extrusion Rate On Morphology and Performance of Polyvinylidene Fluoride Hollow Fiber Membranes Using Polyvinyl Pyrrolidone as an Additive, *Chinese Journal of Polymer Science (English Edition)*, **28(4)**: 527–535 (2010). doi: 10.1007/s10118-010-9054-5.

[6] Mu C., Su Y., Sun M., Chen W., Jiang Z., Remarkable Improvement of the Performance of Poly(vinylidene fluoride) Microfiltration Membranes by the Additive of Cellulose Acetate, *Journal of Membrane Science*, **350(1–2)**: 293–300 (2010). doi: 10.1016/j.memsci.2010.01.004.

[7] Yan L., Li Y.S., Xiang C.B., Preparation of Poly(vinylidene fluoride)(pvdf) Ultrafiltration Membrane Modified by Nano-Sized Alumina (Al2O3) and its Antifouling Research, *Polymer (Guildf)*, **46(18)**: 7701–7706 (2005). doi: 10.1016/j.polymer.2005.05.155.

[8] Zhao X., Liu C., One-Step Fabricated Bionic PVDF Ultrafiltration Membranes Exhibiting Innovative Antifouling Ability to the Cake Fouling, *Journal of Membrane Science*, **515**: 29–35 (2016). doi: 10.1016/j.memsci.2016.05.025.

[9] Zhang Y.Y., Jiang S.L., Yu Y., Xiong G., Zhang Q.F., Guang G.Z., Phase transformation Mechanisms and Piezoelectric Properties of Poly(vinylidene fluoride)/ Montmorillonite Composite, *Journal of Applied Polymer Science*, **123(5)**: 2595–2600 (2012). doi: 10.1002/app.34431.

[10] Wang P., Ma J., Wang Z., Shi F., Liu Q., Enhanced Separation Performance of PVDF/PVP-g-MMT Nanocomposite Ultrafiltration Membrane Based on the NVP-Grafted Polymerization Modification of Montmorillonite (MMT), *Langmuir*, **28(10)**: 4776–4786 (2012). doi: 10.1021/la203494z.

[11] Kotte M.R., Cho M., Diallo M.S., A Facile Route to the Preparation of Mixed Matrix Polyvinylidene Fluoride Membranes with in-Situ Generated Polyethyleneimine Particles, *Journal of Membrane Science*, **450**: 93–102 (2014). doi: 10.1016/j.memsci.2013.08.025.

[12] Rao Kotte M., Hwang T., Han J.I., Diallo M.S., A One-Pot Method for the Preparation of Mixed Matrix Polyvinylidene Fluoride Membranes with in Situ Synthesized and PEGylated Polyethyleneimine Particles, *Journal of Membrane Science*, **474(277–287)**: (2015). doi: 10.1016/j.memsci.2014.09.044.

[13] Causin V., Carraro M.L., Marega C., Saini R., Campestrini S., Marigo A., Structure and Morphology of Solution Blended Poly(vinylidene fluoride)/ Montmorillonite Nanocomposites, *Journal of Applied Polymer Science*, **109(4)**: 2354–2361 (2008). doi: 10.1002/app.28308.

[14] Jian C., Jiding L., Cuixian C., Surface Modification of Polyvinylidene Fluoride (PVDF) Membranes by Low-Temperature Plasma with Grafting Styrene Surface Modification of Polyvinylidene Fluoride (PVDF) Membranes by Low-Temperature Plasma with Grafting Styrene *," (2009). [Online]. Available: http://iopscience.iop.org/1009-0630/11/1/09

[15] Ohno S., Nakata I., Nagumo R., Akamatsu K., Lin Wang X., Ichi Nakao S., Development of Low-Fouling PVDF Membranes Blended with Poly(2-methoxyethyl acrylate) via NIPS Process, *Separation and Purification Technology*, **276**: (2021):
doi: 10.1016/j.seppur.2021.119331.

[16] Wu X., Kang D., Liu N., Shao H., Dong X., Qin S., Microstructure Manipulation in PVDF/SMA/ MWCNTs Ultrafiltration Membranes: Effects of Hydrogen Bonding and Crystallization During the Membrane Formation, *Separation and Purification Technology*, **278**: (2022).
doi: 10.1016/j.seppur.2021.119523.

[17] Wu X., Kang D., Liu N., Shao H., Dong X., Qin S., Microstructure Manipulation in PVDF/SMA/ MWCNTs Ultrafiltration Membranes: Effects of Hydrogen Bonding and Crystallization During the Membrane Formation, *Separation and Purification Technology*, **278**: (2022).
doi: 10.1016/j.seppur.2021.119523.

[18] Valizadeh K., Heydarinasab A., Hosseini S.S., Bazgir S., Fabrication of Modified PVDF Membrane in the Presence of PVI Polymer and Evaluation of its Performance in the Filtration Process, *Journal of Industrial and Engineering Chemistry*, **106**: 411–428 (2022).
doi: 10.1016/j.jiec.2021.11.016.

[19] Mao H., *et al.*, Anti-Fouling and Easy-Cleaning PVDF Membranes Blended with Hydrophilic Thermo-Responsive Nanofibers for Efficient Biological Wastewater Treatment, *Separation and Purification Technology*, **281**: (2022).
doi: 10.1016/j.seppur.2021.119881.

[20] Sivakumar M., Mohan D.R., Rangarajan R., Studies on Cellulose Acetate-Polysulfone Ultrafiltration Membranes: II. Effect of Additive Concentration, *Journal of Membrane Science*, **268(2)**: 208–219 (2006).
doi: 10.1016/j.memsci.2005.06.017.

[21] Lv J., Zhang G., Zhang H., Zhao C., Yang F., Improvement of Antifouling Performances for Modified PVDF Ultrafiltration Membrane with Hydrophilic Cellulose Nanocrystal, *Applied Surface Science*, **440**: 1091–1100 (2018).
doi: 10.1016/j.apsusc.2018.01.256.

[22] Arthanareeswaran G., Sriyamuna Devi T.K., Raajenthiren M., Effect of Silica Particles on Cellulose Acetate Blend Ultrafiltration Membranes: Part I, *Separation and Purification Technology*, **64(1)**: 38–47 (2008).
doi: 10.1016/j.seppur.2008.08.010.

[23] Hossein Razzaghi M., Safekordi A., Tavakolmoghadam M., Rekabdar F., Hemmati M., Morphological and separation Performance Study of PVDF/CA Blend Membranes, *Journal of Membrane Science*, **470**: 547–557 (2014).
doi: 10.1016/j.memsci.2014.07.026.

[24] Razzaghi M.H., Tavakolmoghadam M., Rekabdar F., Oveisi F., Investigation of the Effect of Coagulation Bath Composition on PVDF/CA Membrane by Evaluating Critical Flux and Antifouling Properties in Lab-Scale Submerged MBR, *Water and Environment Journal*, **32(3)**: 366–376 (2018).
doi: 10.1111/wej.12334.

[25] Alias M.H., Hassin N.S., Pui L.P., Misnon I.I., Jose R., "Effect of PVDF-CA Ratio on Electrospun Membrane Fabrication for Water Filtration Application", in *Materials Science Forum*, vol. 981 MSF, Trans Tech Publications Ltd, pp. 356–361 (2020).
doi: 10.4028/www.scientific.net/MSF.981.356.

[26] Pramono E., Simamora A.L., Radiman C.L., Wahyuningrum D., "Effects of PVDF Concentration on the Properties of PVDF Membranes", in *IOP Conference Series: Earth and Environmental Science*, **75(1)**: - (2017).
doi: 10.1088/1755-1315/75/1/012027.

[27] Du C., Ma X., Li J., Wu C., Improving the Charged and Antifouling Properties of PVDF Ultrafiltration Membranes by Blending with Polymerized Ionic Liquid Copolymer P(MMA-b-MEBIm-Br), *Journal of Applied Polymer Science*, **134(17)**: - (2017).
doi: 10.1002/app.44751.

[28] Kumar M., Ulbricht M., Novel Antifouling Positively Charged Hybrid Ultrafiltration Membranes for Protein Separation Based on Blends of Carboxylated Carbon Nanotubes and Aminated Poly(arylene ether sulfone), *Journal of Membrane Science*, **448**: 62–73 (2013).
doi: 10.1016/j.memsci.2013.07.055.

[29] Vadivelan V., Vasanth Kumar K., Equilibrium, Kinetics, Mechanism, And Process Design for the Sorption of Methylene Blue onto Rice Husk, *Journal of Colloid and Interface Science*, **286(1)**: 90–100 (2005).
doi: 10.1016/j.jcis.2005.01.007.

[30] Kumar M., Ulbricht M., Novel Ultrafiltration Membranes with Adjustable Charge Density Based on Sulfonated Poly(Arylene Ether Sulfone) Block Copolymers and their Tunable Protein Separation Performance, *Polymer (Guildf)*, **55(1)**: 354–365 (2014).
doi: 10.1016/j.polymer.2013.09.003.

[31] Basri H., Ismail A.F., Aziz M., Polyethersulfone (PES)-Silver Composite UF Membrane: Effect of Silver Loading and PVP Molecular Weight on Membrane Morphology and Antibacterial Activity, *Desalination*, **273(1)**: 72–80 (2011).
doi: 10.1016/j.desal.2010.11.010.

[32] Jayalakshmi A., Rajesh S., Mohan D., Fouling Propensity and Separation Efficiency of Epoxidated Polyethersulfone Incorporated Cellulose Acetate Ultrafiltration Membrane in the Retention of Proteins, *Applied Surface Science*, **258(24)**: 9770–9781 (2012).
doi: 10.1016/j.apsusc.2012.06.028.

[33] Lapointe J.F., Gauthier S.F., Pouliot Y., Bouchard C., Characterization of Interactions between β-Lactoglobulin Tryptic Peptides and a Nanofiltration Membrane: Impact on the Surface Membrane Properties as Determined by Contact Angle Measurements, *Journal of Membrane Science*, **261(1–2)**: 36–48 (2005).
doi: 10.1016/j.memsci.2005.03.030.

[34] Ike I.A., Zhang J., Groth A., Orbell J.D., Duke M., Effects of Dissolution Conditions on the Properties of PVDF Ultrafiltration Membranes, *Ultrasonics Sonochemistry*, **39**: 716–726 (2017).
doi: 10.1016/j.ultsonch.2017.05.041.

[35] Li J.F., Xu Z.L., Yang H., Yu L.Y., Liu M., Effect of TiO2 Nanoparticles on the Surface Morphology and Performance of Microporous PES Membrane, *Applied Surface Science*, **255(9)**: 4725–4732 (2009).
doi: 10.1016/j.apsusc.2008.07.139.

[36] Woo S.H., Park J., Min B.R., Relationship between Permeate Flux and Surface Roughness of Membranes with Similar Water Contact Angle Values, *Separation and Purification Technology*, **146**: 187–191 (2015).
doi: 10.1016/j.seppur.2015.03.048.

[37] Priya L., Jog J.P., Polymorphism in Intercalated Poly(vinylidene fluoride)/clay Nanocomposites, *Journal of Applied Polymer Science*, **89(8)**: 2036–2040. (2003).
doi: 10.1002/app.12346.

[38] Dillon D.R., Tenneti K.K., Li C.Y., Ko F.K., Sics I., Hsiao B.S., On the Structure and Morphology of Polyvinylidene Fluoride-Nanoclay Nanocomposites, *Polymer (Guildf)*, **47(5)**: 1678–1688 (2006).
doi: 10.1016/j.polymer.2006.01.015.

[39] Ou R., Wang Y., Zhang H., Wang H., Xu T., Preparation of High-Flux Ultrafiltration Membranes by Blending Strongly Charged Polymer, *Journal of Applied Polymer Science*, **134(10)** (2017).
doi: 10.1002/app.44570.

[40] Ahmadizadegan H., Polyester/SiO2 Nanocomposites: Gas Permeation, Mechanical, Thermal and Morphological Study of Membranes, (2020).

[41] Mollayousefi S., Shojaei F., Preparation, Characterization, and Performance Study of PVDF Nanocomposite Contained Hybrid Nanostructure TiO 2-POM Used as a Photocatalytic Membrane, *J. Chem. Chem. Eng. Research Article*, **40(1)**: 35–47 (2021).

[42] Park S.Y., Choi S.H., Chung J.W., Kwak S.Y., "Anti-Scaling Ultrafiltration/Microfiltration (UF/MF) Polyvinylidene Fluoride (PVDF) Membranes with Positive Surface Charges for Ca2+/Silica-Rich Wastewater Treatment, *Journal of Membrane Science*, **480**: 122–128 (2015).
doi: 10.1016/j.memsci.2015.01.041.

[43] An A.K., *et al.*, PDMS/PVDF Hybrid Electrospun Membrane with Superhydrophobic Property and Drop Impact Dynamics for Dyeing Wastewater Treatment Using Membrane Distillation" *Journal of Membrane Science*, **525**:57–67 (2017).
doi: 10.1016/j.memsci.2016.10.028.

[44] Elimelech M., Chen W.H., Waypa J.J., Measuring the Zeta (Electrokinetic) Potential of Reverse Osmosis Membranes by a Streaming Potential Analyzer, *Desalination*, **95**: 269–266 (1994).

[45] Elimelech M., Zhu X., Childress A.E., Hong S., "Role of Membrane Surface Morphology in Colloidal Fouling of Cellulose Acetate and Composite Aromatic Polyamide Reverse Osmosis Membranes," (1997).

[46] Reza A., Reza M., Removal of Nitrate from Water Using TiO 2 / PVDF Membrane Photobioreactor, *J. Chem. Chem. Eng. Research Article*, **40(1)**: 2021 (2021).